Vol.67: e24240601, 2024
https://doi.org/10.1590/1678-4324-2024240601
ISSN 1678-4324 Online Edition

BABT
Brazilian Archives of Biology and Technology

Article - Engineering, Technology and Techniques

Paraconsistent Artificial Neural Network (PANnet) applied to the Detection of (NOx) Nitrogen Oxides Emissions in Petrochemical Combustion Systems

Marcos Carneiro Rodrigues[1]
https://orcid.org/0000-0003-0914-5778

João Inácio da Silva Filho[1*]
https://orcid.org/0000-0001-9715-8928

Arnaldo de Carvalho Junior[2]
https://orcid.org/0000-0002-3417-0062

Hyghor Miranda Côrtes[1]
https://orcid.org/0000-0002-7508-9404

Aldo Ramos Santos[1]
https://orcid.org/0000-0003-0236-1910

Dorotéa Vilanova Garcia[1,3]
https://orcid.org/0000-0002-8769-0328

Mauricio Conceição Mario[1,3]
https://orcid.org/0000-0002-1973-2186

Fábio Giordano[1]
https://orcid.org/0000-0002-6384-9867

Vitor da Silva Rosa[1]
https://orcid.org/0000-0002-5549-7611

Germano Lambert-Torres[1,4]
https://orcid.org/0000-0003-3789-4696

[1]Universidade Santa Cecilia – UNISANTA, Laboratório de Lógica Paraconsistente Aplicada, Santos, SP, Brasil; [2]Instituto Federal de Educação, Ciência e Tecnologia de São Paulo (IFSP), Cubatão, SP, Brasil; [3]Centro Estadual de Educação Tecnológica Paula Souza (CEETPS), São Paulo, SP, Brasil; [4]Instituto Gnarus, Itajubá, Minas Gerais, Brasil.

Editor-in-Chief: Alexandre Rasi Aoki
Associate Editor: Alexandre Rasi Aoki

Received: 10-Jul-2024; Accepted: 23-Sep-2024

*Correspondence: inacio@unisanta.br; Tel.: +55-13- 98128-8298 (JISF)

HIGHLIGHTS

- Paraconsistent Artificial Neural Network-PANNet in Detecting NOx Emissions
- Use of Paraconsistent Logic in Environmental Issues.
- Intelligent Metrology Applied to the Estimation of Nitrogen Oxides.
- Impacts of Gas Emissions on Human Health.

Abstract: The emissions of nitrogen oxides (NOx) that are produced during the combustion of fossil fuels in the petrochemical and metallurgical industries, when combined with other types of pollutants, can have significant impacts on human health and the environment. Therefore, it is essential to investigate techniques that allow the optimization of burning in industrial furnaces with moderate levels of NOx emissions and, for this, computational learning structures that detect and prevent emissions can create efficient AI models. With this objective, we present in this article an Artificial Neural Network-ANN composed of algorithms based on Paraconsistent Annotated Logic-PAL, which is a branch of non-classical logics that deals with situations in which data contains contradictions and inconsistencies in its information. The learning data used was obtained from a 6-burner Vertical Cylinder Industrial Furnace that is in operation in the Oil Refining process

in Brazil. In the data preprocessing phase for training the PANNet structure, real data on the inlet air flow rate during combustion and real fuel flow rate data were used. These values collected in the SCADA system were transformed into normalized degrees of evidence and then applied to the PANNet inputs, creating support patterns for estimating and optimizing the combustion process. The comparative results with a conventional ANN showed that the Paraconsistent Artificial Neural Network-PANNet presents superior performance parameters, thus highlighting its efficiency in creating models that deal with complex modeling problems to estimate industrial NOx emissions in combustion furnaces.

Keywords: Paraconsistent Annotated Logic; Artificial Neural Networks; Machine Learning; Industrial pollution; Nitrogen Oxides; Combustion Furnace.

INTRODUCTION

The global community is increasingly concerned about the impacts of air pollution on human health [1]. Air pollution is present in various places, such as industrial, urban, and agricultural areas. Emissions of different types of pollutants can have adverse effects on human health and the environment, making it essential to adopt optimization techniques in production to control and reduce these emissions [2]. The increasingly poor air quality has directly generated health hazards for urban residents and in a highly polluted area, the emissions produced during the combustion of fossil fuels can be a dangerous disease transmission factor [3].

In industrial processes that involve heating and combustion, it is necessary to raise the temperature of certain materials or substances to achieve the desired results. These operations typically occur in controlled environments such as furnaces, reactors, or boilers and require a large amount of energy, often provided by burning fossil fuels [3,4].

The release of carbon dioxide (CO_2), one of the main greenhouse gases occurs in the combustion of fossil fuels, and generates various pollutants, including nitrogen oxides (NOx), fine particles (PM2.5 and PM10), volatile organic compounds (VOCs), and black carbon. These pollutants are common byproducts of high-temperature combustion [4].

Nitrogen Oxides (NOx) Emissions and Industrial Furnace

The petrochemical and metallurgical industries face a serious problem of causing levels of environmental pollution through emissions of nitrogen oxides (NOx), which is a family of chemical compounds that include nitric oxide (NO) and nitrogen dioxide (NO2). NOx emissions that are produced during the combustion of fossil fuels, when combined with other types of pollutants, can have significant impacts on human health and the environment, as they are responsible for the acidity of rain, reduction of the ozone layer and formation of photochemical oxidants. Therefore, it is essential to investigate techniques that allow the optimization of burning in industrial furnaces with moderate levels of NOx emissions [3][5].

The operation of an industrial furnace is based on the theory of combustion systems, which relies on the interaction of three crucial elements: a) the fuel source; b) the oxidizing agent (or oxidant); and c) the energy source needed to initiate the reaction. The flame is produced by the controlled combination of these elements, and the combustion process is meticulously managed to ensure efficiency and safety, as well as compliance with environmental regulations [5].

Playing a critical role in various processes, industrial furnaces must operate at maximum efficiency to ensure optimal transfer of heat generated to the processing load. The quality of such combustion systems can be indicated by the amount of air present, as a balanced concentration of oxygen is crucial for effective combustion. If oxygen becomes scarce, incomplete combustion may occur, leading to inefficient energy use and the production of toxic gases. On the other hand, an excess of oxygen in the combustion chamber can result in a decrease in the Adiabatic Flame Temperature (AFT), limiting the thermal efficiency of the process [6,7].

Compliance with regulatory controls necessitates maintaining the combustion gas output at a specific set-point (SP). To achieve this goal, it is often necessary to adjust the fuel flow rate; however, this adjustment can increase not only the operational costs of the furnace but also the production of gases generated in the combustion reaction. These gases must be properly managed to minimize environmental impact [7].

This study aims to address the identification of the influence of input parameters on the presence of NOx based on emissions generated in industrial furnaces and, this is made by computational learning structure that detect and prevent emissions. By focusing on identifying NOx production, valuable insights can be obtained regarding combustion performance and emissions, enabling predictions about the intensity of these

emissions. These predicted data based on inputs to the industrial furnace can contribute to the development of more precise and adaptable control measures, resulting in safer and more sustainable operations with controlled industrial emissions in industrial furnaces based in efficient AI models [8].

The main objective of this work is to develop a methodology that can identify and predict the presence of NOx based on emissions generated during industrial heating processes, using the inputs utilized. This methodology is structured around paraconsistent logic [9], a branch of mathematical logic that, unlike classical logic, allows for the manipulation and coexistence of contradictions within the same inference system. It is expected that this approach will contribute to the development of more efficient and sustainable strategies for managing emissions in industrial combustion processes. Therefore, in this work, a computational system model was implemented, dedicated to identifying the intensity of NOx emissions and estimating an optimized process in an industrial furnace based on a structure configured with Artificial Neural Networks (ANN) using algorithms based on PAL2v [9,10].

Paraconsistent Annotated Logic with annotation of two values (PAL2v

Paraconsistent Logic (PL) was created to oppose some binary principles that support Classical Logic, including non-contradiction and thus deal with contradictory signals [9] [11].

Paraconsistent Annotated Logic with annotation of two values (PAL2v) is an extension of PL and therefore belongs to the family of non-classical logics. As propositional and evidential logic, a paraconsistent logic signal in PAL2v is represented by a proposition P accompanied by an annotation (μ,λ). The annotation always consists of degrees of favorable evidence μ and unfavorable evidence λ, both contained in the interval 0≤(μ,λ)≤1, and belonging to the set of real numbers $\Re$ [12,13]. By associating PAL2v in a four-vertex lattice, it is possible to obtain equations that allow the treatment of complex data with incomplete and contradictory information. These fundamental PAL2v equations will be shown below.

The equation (1) allows for the calculation of the degree of certainty D_C [9].

$$D_C=\mu-\lambda \tag{1}$$

When D_C = -1, it determines the logical value false **F** for proposition P. When D_C = 1, it determines the logical value true **t** for proposition P.

The value of the degree of contradiction D_{CT} is given by equation (2):

$$D_{CT}=\mu+\lambda-1 \tag{2}$$

When two sources of favorable and unfavorable evidence have high values, a degree of contradiction D_{CT} will determine the contradictory logical state Inconsistent (T), with D_{CT}=1. However, the absence of both favorable and unfavorable evidence simultaneously will lead the proposition to a paraconsistent logical state Paracomplet (⊥), where D_{CT}=−1.

The internal point into associated PAL2v-lattice composed by *D*c and *D*ct is considered a paraconsistent logical state ϵτ [9][14,15]. Therefore:

$$\epsilon\tau(Dc,Dct) \tag{3}$$

Segment *d* represents the distance from the point ϵτ(*D*c,*D*ct) to the nearest logical endpoint, namely True (t) or False (F). The value of *d* is given by the equation (4):

$$d=\sqrt{(1-D_C)^2+D_{CT}^2} \qquad 0\le d\le 1 \tag{4}$$

The degree of real certainty, denoted as D_{CR}, is given by the equations (5) and (6) and removes the effects of contradiction.

$$D_{CR}=1-d \tag{5}$$

If D_C >0

$$D_{CR}=d-1$$

If D_C <0 (6)

As D_C and D_{CR} are normalized according to the input, then they can be used together with other sources of information to create Paraconsistent Analysis Networks (PANets). New parameters should be established that are normalized within the same interval as μ and λ.

Figure 1a shows the Lattice associated with PAL2v with the main results obtained by the interpretations shown in the basic equation.

Equations (7) and (8) establish a linear relationship of μ_E with the sources of evidence μ and λ. However, the dependency condition of D_{CR} on the sign of D_C, as well as the existence of the saturation condition of d at the unit value, introduces nonlinearities in the D_{CR} parameter [14-19].

$$\mu_E = \frac{D_C + 1}{2} \tag{7}$$

$$\mu_{ER} = \frac{D_{CR} + 1}{2} \tag{8}$$

Therefore, the output of a PANNet should include the values of the resulting certainty degree μ_E and resulting real certainty degree μ_{ER} [9].

As seen in [10] and [20] with these basic equations, the PAN algorithm – Paraconsistent Analysis Node was created. Configurations structured in PAN interconnections were used in several studies to classify and process data originating from uncertain knowledge.

Figure 1b shows the symbol representing the PAN with its two outputs μE and μER.

The PAN algorithm is the core of the functional blocks called paraconsistent artificial neural cells (PANCell). In general, paraconsistent cells (PANCells) are algorithms that complement PAN with additional rules, decisions and equations based on PAL2v.

A typical PANCell can be defined as a block with functional arrangement in the PAN algorithm such that it will have the output value μE at sampling time k+1 which depends on the value at input μ and output μE at sample k. Therefore, as seen in [12] this Neural cell exhibits a delayed response or integration effect that can be achieved through equation (9).

$$\mu_{Ek} = \frac{\mu_k + \mu_{E(k-1)}}{2} \tag{9}$$

In the work developed in [15,16] and [17] it was demonstrated that a PAN meets two requirements so that it can be considered a trainable neuron and thus compose a neural network: 1. it is a non-linear function; 2. its function may be derivable. Based on considerations of these concepts, PAN was used as an artificial neuron forming a configuration of paraconsistent Artificial neural network structures (PANNet) where weights are applied between connections (synapses) resembling traditional ANNs. In this process, PANNets and their derivatives of the PAL2v activation function were trained.

The PAL2v equations for the derivatives are [15-17]:

For D_C positive ($\mu > \lambda$)

$$\frac{\partial \mu_{ER}}{\partial \mu} = \frac{(1-\mu)}{(2\mu^2 + 2\lambda^2 - 4\mu + 2)^{0.5}} \tag{10}$$

$$\frac{\partial \mu_{ER}}{\partial \lambda} = \frac{-\lambda}{(2\mu^2 + 2\lambda^2 - 4\mu + 2)^{0.5}}$$

For D_C negative ($\mu < \lambda$)

$$\frac{\partial \mu_{ER}}{\partial \mu} = \frac{\mu}{(2\mu^2 + 2\lambda^2 - 4\lambda + 2)^{0.5}} \tag{11}$$

$$\frac{\partial \mu_{ER}}{\partial \lambda} = \frac{\lambda - 1}{(2\mu^2 + 2\lambda^2 - 4\lambda + 2)^{0.5}}$$

Figure 1c shows the Neuron-PAL2v symbol with representations of the result of the derivatives that will act as feedback to adjust the weights in the training phase.

In this work a computational system model was implemented, dedicated to identifying the intensity of NOx emissions and estimating an optimized process in an industrial oven based on a structure configured

with Artificial Neural Networks (ANN) using algorithms based on PAL2v. This type of computational structure was called Paraconsistent Artificial Neural Network (PANNet) and was initially presented in [10] in the form of a unique algorithm that makes up a Paraconsistent Artificial Neural Learning Cell [lPANcell]. From this initial work, other configurations were developed, such as the computational structures for Learning from demonstration seen in [14] and [18]. In other works, as can be seen in [15] and [17], PANNets were published structured in algorithm configurations similar to lPANcell, but composed of hidden layers and adapted for backpropagation learning, which allowed comparisons of results with conventional ANN.

Figure 1d shows a typical configuration of a PANNet used in [15].

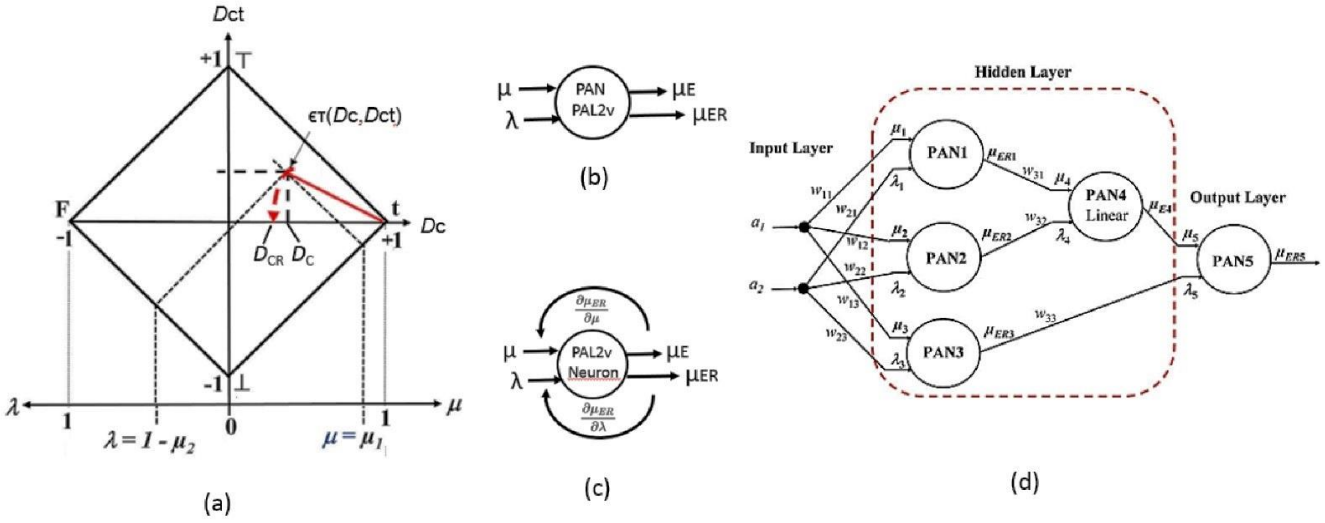

Figure 1. Representation of PAL2v algorithm symbols. a) Lattice Associated with PAL2v with the main resulting values. a) PAN - Paraconsistent Analysis Node. c) PAL2v Paraconsistent Neuron. w). d) Structure of a typical PANNet.

Levenberg-Marquardt method

This article deals with a PANNet structure with PANCells similar to those presented in [15] and [17] with a Levenberg-Marquardt Algorithm [21] adapted for processing information data on the presence of NOx in emissions generated in industrial furnaces [9]. The Levenberg-Marquardt method can be described as an approximation of the Newton method, used for training neural networks, where the error is associated with an expression containing second-order derivatives [8][21]. The weight update is given by the equation (12):

$$w_{k+1} = w_k - \frac{J^T E}{J^T J - \omega I} \tag{12}$$

Where:

1. wk represents the current weights,
2. J is the Jacobian matrix of the network,
3. ω is the damping parameter,
4. I is the identity matrix,
5. E is the error vector.

The product ωI determines how much the weights are adjusted to minimize the error. If the updated weights increase the MSE (Mean Square Error), the value of ω should be increased by multiplying it by a factor β, typically around 10, and then the weight update calculation should be repeated. If the error decreases with the newly applied weights, these replace the previous weights, and the value of ω is divided by β [21]. The algorithm is stopped if it meets certain stopping criteria, which may include:

1. The error falls below a predefined threshold.
2. The gradient of the error function becomes sufficiently small.
3. A maximum number of iterations or epochs is reached.
4. The changes in the error or weights between successive iterations are below a specified threshold.

MATERIAL AND METHODS

The computational structure of Artificial Neural Networks (ANN) using algorithms based on Annotated Paraconsistent Logic, called PANNet, was built to identify the intensity of NOx emissions and estimate an optimized process in an industrial furnace of an oil company. To build PANNet structure, the following steps were carried out:

1. Data acquisition from a real system and preprocessing procedures for value normalization.
2. Construction of a computational ANN structure operating with algorithms based on PAL2v, capable of relating input parameters to NOx emissions, creating support patterns for the estimation and optimization of the combustion process.
3. Development of a Levenberg-Marquardt Algorithm adapted to a computational ANN structure operating with algorithms based on PAL2v.
4. Created conditions for comparative tests between conventional ANNs and the constructed paraconsistent ANN were conducted.

Data Preprocessing

The data used in this research were obtained from a Vertical Cylinder type industrial furnace with convection, powered by 6 burners, with preheating of the primary air through heat exchange with the generated combustion gases. In the data collection was carried out considering the operation of the industrial furnace in a steady-state regime, with values obtained over a 5-minute sampling period during continuous operation. In the data preprocessing phase for training the PANNet structure, real data on the inlet air flow rate during combustion and real fuel flow rate data were used. These values collected in the SCADA system were transformed into normalized degrees of evidence and then applied to the PANNet inputs, creating support patterns for estimating and optimizing the combustion process.

In the preprocessing phase, the acquired data were arranged in a matrix format, with each sample placed in rows and the variables in columns. During this preprocessing procedure, null and negative values were removed. After the preprocessing phase, where data adequacy occurred, the collected data represented by D_S were then normalized according to equation (13), ensuring that within the entire discourse universe, their values were limited to the closed interval [0,1], thus aligning with the limits of the evidence degrees μ and λ of PAL2v.

$$d_{S_{i,j}} = \frac{\left(D_{S_{i,j}} - \min\left(\boldsymbol{D_{s_j}}\right)\right)}{\max(\boldsymbol{D}_j) - \min\left(\boldsymbol{D_j}\right)} \tag{13}$$

Where,

1. $d_{Si,j}$ is the i-th element of the j-th variable in the normalized dataset.
2. $D_{Si,j}$ is the i-th element of the j-th variable in the original dataset.
3. i represents the i-th sample of the dataset.
4. j represents the j-th variable to be normalized.
5. min (D_j) is the minimum value of the j-th variable in the dataset.
6. max (D_j) is the maximum value of the j-th variable in the dataset.

The variables chosen as input for the PANNet were the inlet air flow rate used in combustion (A) and the fuel flow rate (B). The production of NOx was selected as the output parameter.

The flowchart detailing the data collection phase in the SCADA system, followed by preprocessing and the mathematical procedure for transforming the values of the physical quantities into degrees of evidence using equation (13), is shown in Figure 2.

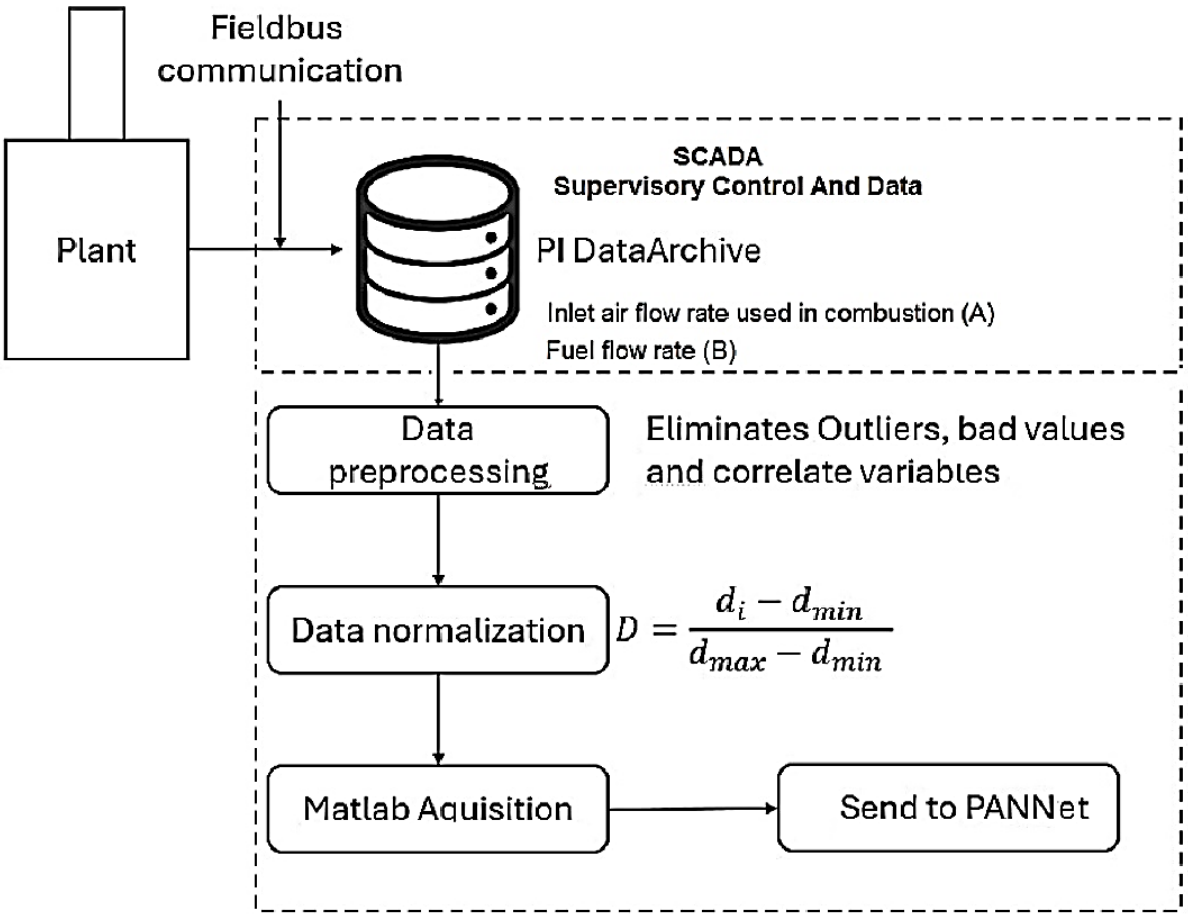

Figure 2. Flowchart detailing the data collection phase and the mathematical procedure for obtaining the normalized degrees of evidence.

PANNet Structure

The strategy adopted in the research was to use only neurons with nonlinear output. To achieve this, the number of inputs to neurons in the subsequent layer is adjusted. Considering the total number of neurons in the previous layer (n_{l-1}) and the number of gates (n_P) of neurons in the subsequent layer (n_l), equation (14) establishes that:

$$n_{p;l} = 2^{\lceil \log_2(n_{l-1}) \rceil} \tag{14}$$

Where $\lceil \log_2(n_{l-1}) \rceil$ is the ceil of $\log_2(n_{l-1})$.

Being μ_j and λ_j respectively, the inputs corresponding to degrees of favorable and unfavorable evidence, μ_i is defined as any input of the Paraconsistent Neuron, considering parity.

The equation (15) defines the linear output $\mu_{E(N-1)}$, where N is the number of gates of the Paraconsistent Artificial Neural Networks (PANNet).

$$\mu_{E\,N-1} = \frac{1}{2N}\sum_{j=1}^{n_p}(-1)^{i+1}(\mu_i) + \frac{1}{2} \tag{15}$$

It is proposed that the output of the paraconsistent neuron be nonlinear, and for this purpose, a PAN with output μ_{ER} is used as the activation function, with a bias λ_B =0.5. generalizing the equations for the partial derivatives of μ_{ER} with respect to the inputs of a paraconsistent neuron with n_p inputs, according to equation (16), where $(-1)^{i+1}$ defines the sign alternation based on the parity of i, representing the index of the neuron's input.

$$\frac{\partial \mu_{ER}}{\partial \mu_i} = (-1)^{i+1} \frac{(1-\mu_E)\sqrt{2\mu_E^2-4\mu_E+\frac{5}{2}}}{2N\left(2\mu_E^2-4\mu_E+\frac{5}{2}\right)} \quad \text{if } \mu_{EN-1}>0.5 \tag{16}$$

$$\frac{\partial \mu_{ER}}{\partial \mu_i} = (-1)^{i+1} \frac{\mu_E\sqrt{2\mu_E^2+\frac{1}{2}}}{N^*(4\mu_E^2+1)} \quad \text{if } \mu_{EN-1}<0.5$$

$$\frac{\partial \mu_{ER}}{\partial \mu_i} = (-1)^{i+1} 0.5 \quad \text{if } \mu_{EN-1}=0.5$$

Considering that neurons in a PANNet require inputs to be normalized within the interval [0,1], it has been established that the algorithm will describe an input μ_{ji} for any neuron N_i receiving an output $A_{j;l-1}$ from neuron N_j in the previous layer, combined with a weight $W_{ij\{l\}}$. This description follows equation (17):

$$\mu_{ji;l} = \max\left[0, \min\left(1, W_{ij;\{l\}} * A_{j;l-1}\right)\right] \tag{17}$$

Where,

1. $\mu_{ji;l}$ is the j-th input of the i-th neuron in the layer l
2. $W_{ij;\{l\}}$ is the j-th weight between the i-th neuron in the layer l and the j-th neuron in the previous layer
3. $A_{j;l-1}$ is the output of the j-th neuron of previous layer

Therefore, the forward propagation algorithm is defined according to the following sequence:

1. Determine the total number of layers L.
2. Determine the number of neurons for each layer l.
3. Determine the number of gates for neurons N_i.
4. Establish the criterion for input saturation of N_i.
5. Calculate $\mu_{E;l}$, $\mu_{ER;l}$, and $\partial\mu_{ER;l}$.
6. Repeat steps 2 to 5 until the output layer neuron is reached.

For training the PANNet structure, the approach considered in the literature involved the use of PAL2v in neural networks (NNs). In this study, data collected from industrial furnace, comprising 360 sampling points, were randomly recombined to avoid sequence bias during training. Therefore, the training algorithm used in this research was Levenberg-Marquardt, allowing training on the entire dataset per training epoch.

The algorithm construction sequence used in this study is as follows:

1. Establish the stopping criteria ε_1, ε_2 and ε_3.
2. Initialize the parameter β.
3. For the nth input, perform forward propagation to compute the nth output y and establish the column vector Y.
4. Set the Mean Squared Error (MSE).
5. Find the partial derivatives $\partial y/\partial W$ and establish the row vector P.
6. Establish the Jacobian matrix (J), the Hessian matrix H, and the function ω.
7. Set the row vector P_{K+1}.
8. Calculate the new MSE value and compare it with the old MSE.

    - 8.1 If $MSE_{K+1} \geq MSE_K$, increase the value of β and return to step 5.
    - 8.2 If $MSE_{K+1} < MSE_K$, update the weights, revert the value of β, and return to step 3.
    - 8.3 If ε_1, ε_2, or ε_3 are satisfied, stop.

Figure 3 shows the architecture of the PANNet used, where X_1 is the fuel flow rate and X_2 is the air flow rate. It can be seen that X_1 and X_2 combine to create a third input, X_1X_2, to add nonlinearity to the network. The hidden layer consists of three neurons H_1, H_2 and H_3, while the output layer consists of one neuron Y. The weights are initialized randomly within the range [0,1]. All neurons are paraconsistent types with a nonlinear output.

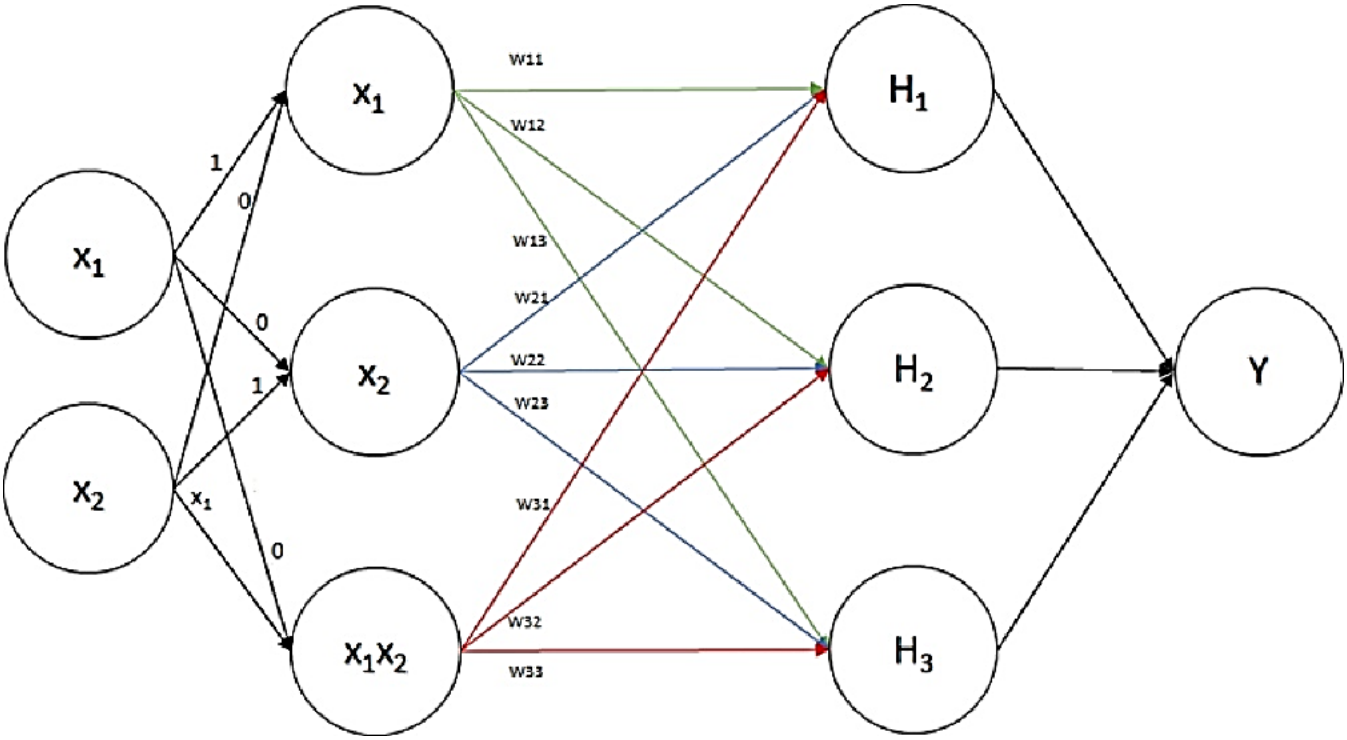

Figure 3. PANNet Architecture.

For a comparative analysis to demonstrate the efficiency of the proposed PANNet structure in this research compared to commonly used ANNs, various tests were applied using the real data described at the beginning of the chapter. The comparison was made between the two types of artificial neural networks, with the main reference being the configuration of a network that uses the log-sigmoid function.

RESULTS AND DISCUSSION

The results obtained from the simulations conducted on the two types of networks configured for the simulation tests are presented below. Initially, Figure 4 shows the graphs that represent the performance comparison of the two distinct neural networks in relation to the activation functions used.

It is observed that the first network uses the PAN cell, while the second incorporates the Log-Sig function. It is noticeable that both networks can track abrupt variations relative to the target. This characteristic is visualized due to the randomness of the data. However, a better adjustment of the PANNet is perceived compared to the Log-Sig Network.

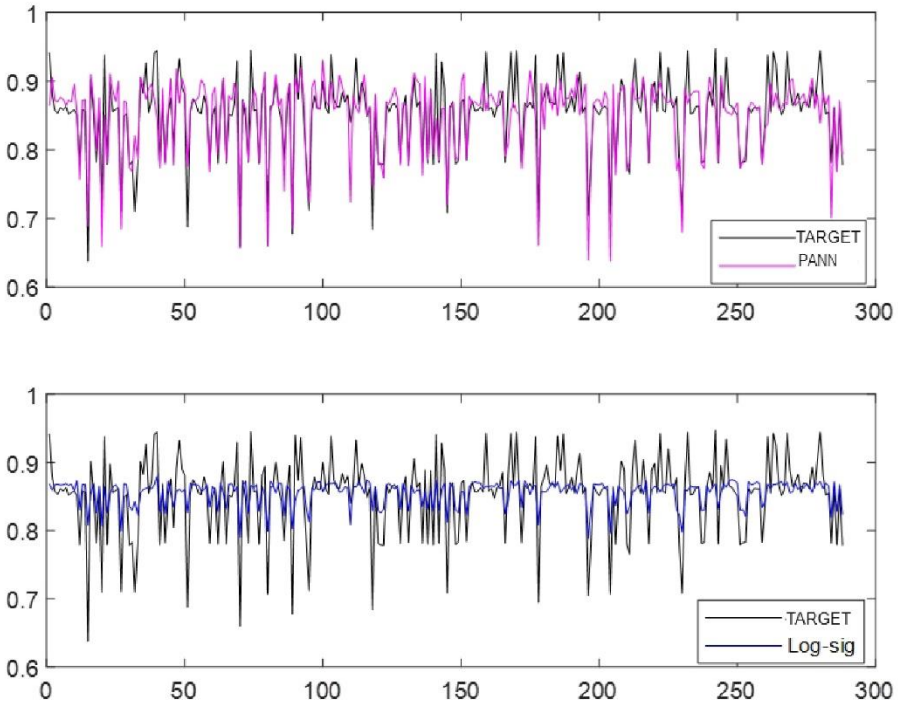

Figure 4. Comparison of the Behavior of Neural Networks with Log-Sigmoid Activation Functions and PANNet.

Figure 5a shows the evolution of the MSE throughout the training process for both neural networks. Notably, the neural network with the log-sigmoid function started with a lower initial MSE compared to the paraconsistent network. However, over the epochs, a trend reversal is observed. The PANNet surpassed the log-sigmoid, achieving a significantly lower MSE by the end of the training. Around epoch 15, the network stabilized its MSE, suggesting that initially, the PANNet had more difficulties adjusting to the data. However, its ability to overcome this initial disadvantage and achieve a lower MSE by the end of the training indicates a remarkable capacity for adaptation.

Figure 5b shows the comparison of the error histograms between the log-sigmoid neural network and the PANNet. It can be observed that the PANN maintained the error concentrated near the zero-error region, while the log-sigmoid neural network had its errors more distributed in the negative error region.

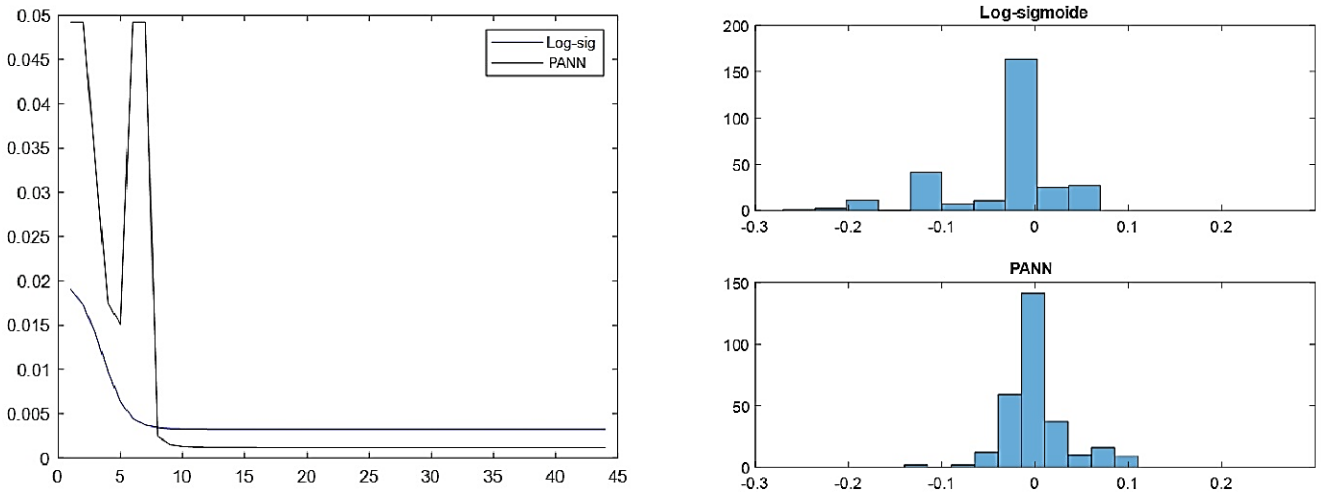

(a) (b)

Figure 5. Performance Results of PANN: (a) MSE Comparison; (b) Error Histogram.

It can be observed that the PANNet exhibits characteristics close to a normal distribution. This indicates that the errors are symmetrically distributed around a mean value (usually close to zero). This suggests that the model is well-fitted to the data since the errors are balanced, with equal probability of being positive or negative and there is no systematic bias in the errors, indicating that the network is not consistently underestimating or overestimating the output values.

Figure 6 shows the comparison of output values using the PANNet, fed with inputs independent of the training set, equivalent to 20% of the total data set. For values distributed randomly, the PANNet was able to track the changes in the real output values.

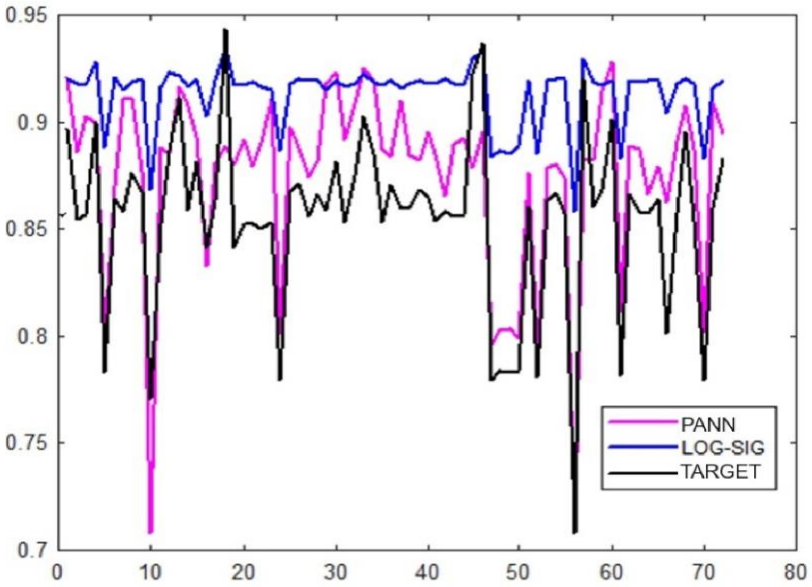

Figure 6. Network Validation.

In Figure 7, the data is rearranged in temporal order, and the PANNet is tested again. A deviation of approximately ±0.05 between the temporal output and the PANNet was observed. Overall, it is noted that the PANNet tends to maintain a stable error for outputs with values that do not vary sharply, yet it is capable of correcting abrupt variations.

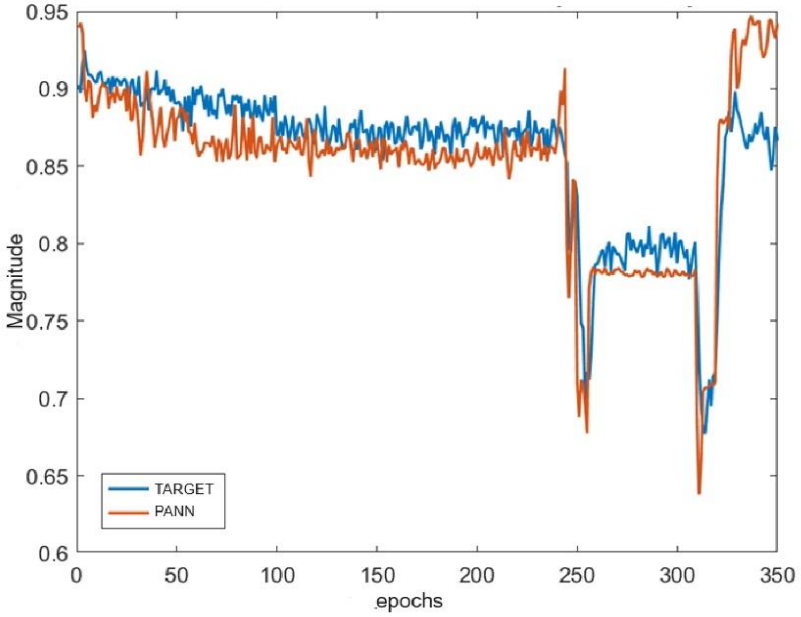

Figure 7. Comparison of PANNet and target over time.

In Figure 8a, it was shown that the Log-Sigmoid Network constructs surfaces where there is a sharp variation in values. Moreover, for both fixed variable X_1 and variable X_2, the curve will be increasing, indicating

that both fuel and air flow variables favor NOx production. The lack of intersection between surfaces indicates that the Log-Sigmoid Network did not detect interaction between the variables.

In Figure 8b, the behavior is shown to be increasing for X_1 and decreasing for X_2, and Table 1 displays the training weight values of the PANNet. The forward propagation test performed with the weights applied to the PANNet, comparing the behavior in Figure 8b with Table 1, indicates that the nature of the network cannot be confirmed solely by observing the weight values. The input X_2, which corresponds to the airflow rate in the presented problem, had high weights for hidden layers 2 and 3, being an even (negative) input.

However, the propagation from the hidden layer to the output layer makes the higher influence of X_2 positive relative to the output, as shown in the 2nd row of the 5th column in Table 1, which illustrates how the weights propagate through the network. The input X_1, which is the fuel flow rate, was related to the odd inputs but had its weights negatively influenced by both the subsequent layer and the combined input X_1X_2.

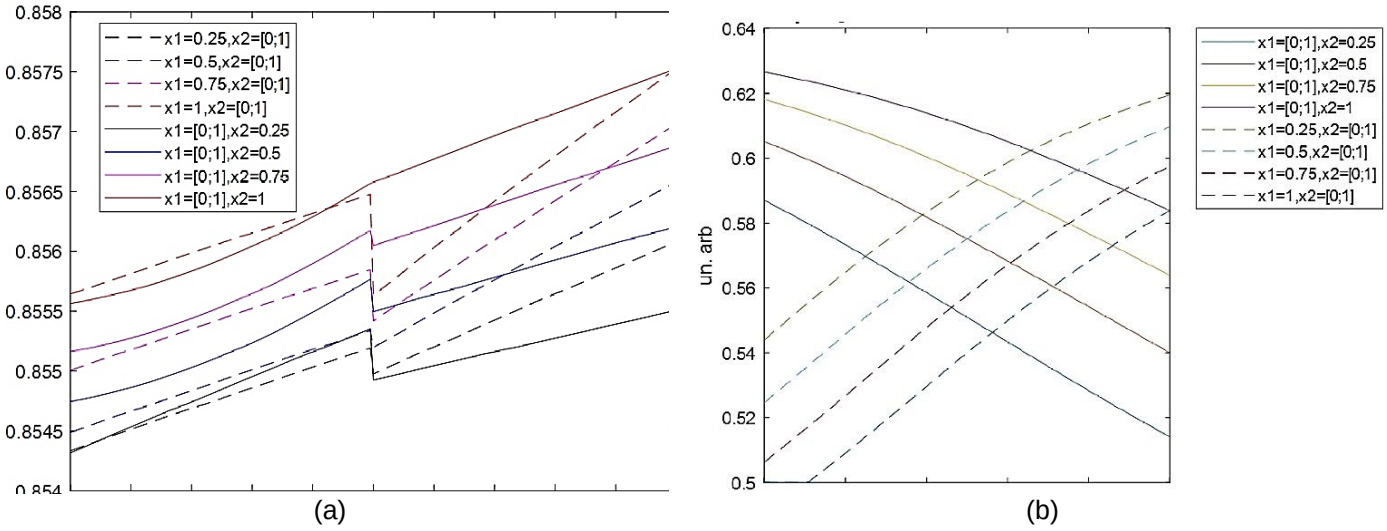

Figure 8. Comparison of output for different input values. (a): Log-sig. (b): PANNet.

Table 1. Relationship of Input Influence Propagated by PANNet.

Inputs	**H_1**	**H_2**	**H_3**	**H_1Y_1**	**H_2Y_1**	**H_3Y_1**
X_1	(+)0.5806	(+)0.2989	(+)0.7137	(+)0.4211	(-)0.2725	(+)0.0616
X_2	(-)0.3605	(-)0.7185	(-)0.9953	(-)0.2614	(+)0.6553	(-)0.0860
X_1X_2	(+)0.0837	(+)0.46820	(+)0.0938	(+)0.0607	(-)0.4270	(+)0.0081
Inputs	**H_1**	**H_2**	**H_3**	**H_1Y_1**	**H_2Y_1**	**H_3Y_1**
X_1	(+)0.5806	(+)0.2989	(+)0.7137	(+)0.4211	(-)0.2725	(+)0.0616
X_2	(-)0.3605	(-)0.7185	(-)0.9953	(-)0.2614	(+)0.6553	(-)0.0860

It appears that the Zeldovich mechanism indicates that the combustion air temperature AFT influences T-NOx formation. Since an excess of O_2 reduces the temperature, a decrease in T-NOx production is expected as O_2 increases. However, X_2 represents the air flow, which contains approximately 79% of N_2, contributing to NO_x formation through its decomposition.

Figure 8b shows a stabilization of NO_x production as X_2 increases, attributed to the decrease in AFT due to the input of air. Regarding fuel, while it helps increase AFT, an excessive amount can lead to the formation of other gases (CO, CO2). Increasing fuel consumption utilizes oxygen for the production of these gases, creating a deficit for NOx formation.

In Figure 8b, it is also evident that increasing fuel causes NOx formation to decrease gradually due to higher AFT. As the mixture becomes rich, combustion becomes incomplete, leading to a decrease in AFT and the formation of CO. This behavior can be observed in the steepening of the curves beyond a certain point of X_1 growth.

In Figure 8b, it was shown that the nonlinearity induced by the third input neuron is not capable of generating intersection points on the level curves shown.

The trained PANNet was thus unable to demonstrate traces of synergy between Fuel and Air for NOx production. This result can be anticipated by analyzing the weights of X_1X_2 in Table 1, where it is observed that their values are significantly lower compared to the others, despite being in the same order of magnitude.

This indicates that the nonlinear nature of the NOx production reactions was detected, although they were not able to demonstrate synergy.

The observations in Figure 8b can be compared with the distribution of minor species as the combustion mixture's richness increases [7], as shown in Figure 9, which represents the formation of NO.

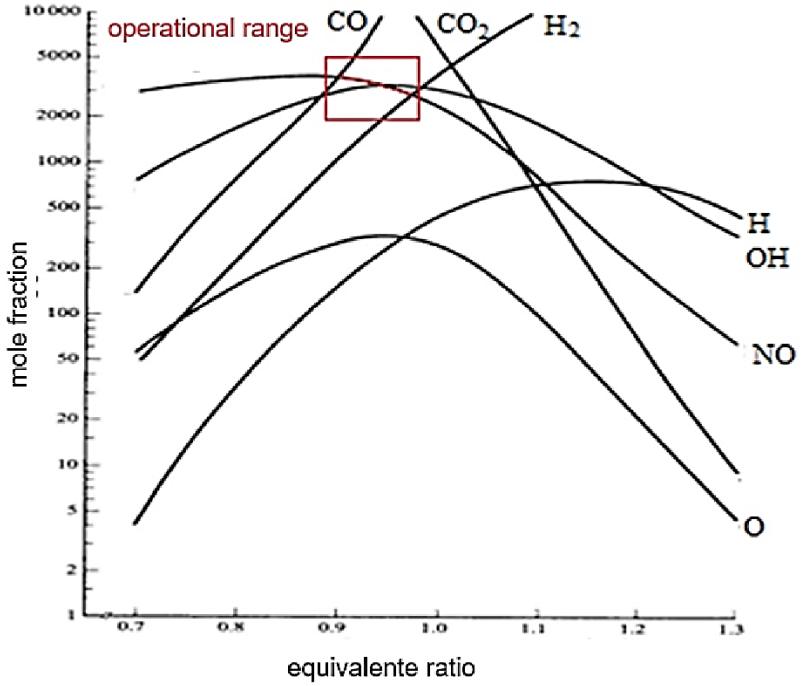

Figure 9. Relationship between distribution of minor chemical species relative to the Fuel/Air ratio [7].

The computational structure built with the PAL2v-sigmoid output function was able to reproduce nonlinearities while the single bias used in the neuron served to maintain its continuity.

The "additive" function was capable for admitting subtraction operations, ensuring that the weights always remained within the interval [0,1]. With this form of computational structure, there was also an adjustment in obtaining the additive function "μ_E", where the internal PAN Cells receive the unfavorable degree of evidence in a complemented manner. Thus, it was possible to establish a general formula for any number of inputs, always preserving the model for "2N" inputs.

It was found that with the new additive function associated with the continuity bias, the derivative of the activation function no longer has discontinuities and is also differentiable over the entire interval [0,1]. This means that the possibility of deriving the output function in the second order allows for the use of Hessian matrices, enabling the application of the Levenberg-Marquardt method for PANNet learning.

CONCLUSION

Industrial emissions refer to by-products released during production and manufacturing processes in industries. Nitrogen oxide (NOx) emissions, which occur most notably in the chemical, petrochemical, and metallurgical industries, have become a significant concern in the context of environmental pollution. Therefore, investigations aiming to find more efficient computational models that can bring new techniques for NOx detection are becoming increasingly important, providing industries with the means to optimize their processes and reduce emissions. Considering this problem, the present work presented a computational modeling capable of estimating the intensities of nitrogen oxide (NOx) emissions in an industrial vertical cylindrical furnace with 6 burners. The detection model involved configurations of Artificial Neural Networks built with algorithms based on Paraconsistent Logic, which is a branch of logic that deals with situations where there are contradictions and inconsistencies in the data. Unlike classical logic, which assumes that all propositions are either true or false, paraconsistent logic allows for dealing with information that can be simultaneously true and false, or whose truthfulness cannot be conclusively determined. And so, for the detection of nitrogen oxide (NOx) emissions, paraconsistent algorithm structures were formed, composing PANNet models using neurons whose weights between synapses are adjusted as they learn to detect the output from the input data. In general, it was found that the paraconsistent model built with the PANNet showed a significant increase in efficiency in the task of NOx detection. Additionally, among the beneficial

features presented, its ability to make the network learn the output from a dataset instead of learning a single output from a set of inputs stands out. This allowed for better generalization of the target function from the input dataset.

Comparing the performance of the model built with the PANNet to that built with the conventional log-sigmoid network, which was also subjected to the Levenberg-Marquardt method, it was found that although the PANNet showed a less favorable start, its results improved over the course of learning. The obtained and compared values showed that the model built with the PANNet had a lower MSE than the Log-Sigmoid, thus being more efficient. Therefore, the model built with the PANNet algorithms proved to be more suitable for supporting computational architectures in NOx detection systems for the optimization of industrial furnaces.

Funding: This research received no external funding
Conflicts of Interest: The authors declare no conflict of interest.

REFERENCES

1. Pepplow LA, Silva VL, Betini RC, Pereira TCG. Evaluation of Global Heating Reduction Potential with the Replacement of Electricity Supplied by the Local Concessionaire Via Solar Renewable Source. Braz Arch Biol Technol. 2019. 62(spe), e19190003. https://doi.org/10.1590/1678-4324-smart-2019190003
2. Yu C, Hui S. Research on Value Assessment and Compensation for Health Hazards of Urban Air Pollution-A Case Study of Urumqi. Braz Arch Biol Technol. 2016. 59(spe), e16160503. https://doi.org/10.1590/1678-4324-2016160503
3. Li YX, Zhao FJ, Yu DD. Effect of nitrogen limitation on cell growth, lipid accumulation and gene expression in Chlorella sorokiniana. Braz Arch Biol Technol, 2015. 58(3), 462–467. https://doi.org/10.1590/S1516-8913201500391
4. Zhenhai D. Varied Slope Rules Self Adaptive Fuzzy Control Algorithm of Crude Oil Heating. International congress on educational information technology. 2010. pp: 122－124, China September, 2010
5. Blair TH. Fossil Fuels and The Basic Combustion Process, in Energy Production Systems Engineering, IEEE, 2017, pp.107-22, https://doi.org/10.1002/9781119238041.ch4
6. Kutlumukhamedov AR, Skiba DV, Bakirov FG. Combined Method for Prediction of Carbon Monoxide Emission from Gas Turbine Combustion Chambers. 2021. pp. 1-4. https://doi.org/10.1109/EC52789.2021.10016861
7. Turns SR. An Introduction to Combustion. 3rd ed. 2013. New York: McGraw-Hill Education.
8. Khan K, Sahai AA. Comparison of BA, GA, PSO, BP and LM for Training Feed forward Neural Networks in e-Learning Context. I.J. Intelligent Systems and Applications, 2012, 7, 23-9.
9. Da Silva Filho JI, Lambert-Torres G, Abe JM. Uncertainty Treatment Using Paraconsistent Logic: Introducing Paraconsistent Artificial Neural Networks; Frontiers in Artificial Intelligence and Applications; IOS Press: Amsterdam, The Netherlands, 2010; Volume 211, p. 328.
10. Salinas CT, Castilho T, Da Silva Filho JI, Marcelo-Aldana D. Alkaline gases emission estimation and paraconsistent logic techniques application to label bagasse combustion conditions, Therm Sci Eng Prog. 2023;40:101773, ISSN 2451-9049, https://doi.org/10.1016/j.tsep.2023.101773
11. De Carvalho Junior A, Justo JF, Oliveira AM, Da Silva Filho JI. A comprehensive review on paraconsistent annotated evidential logic: Algorithms, Applications, and Perspectives, Eng. Appl. Artif. Intell. 2024;127(B):107342, ISSN 0952-1976, https://doi.org/10.1016/j.engappai.2023.107342
12. Côrtes HM, Santos PE, Da Silva Filho JI. Monitoring electrical systems data-network equipment by means of Fuzzy and Paraconsistent Annotated Logic. Expert Syst. Appl. 2021, 187, 115865. https://doi.org/10.1016/j.eswa.2021.115865
13. Côrtes HM, Santos PE, Da Silva Filho JI, Cubic Paraconsistent Analysers with Evidence Filter and Temporal Analysis. Expert Syst Appl, 2023;230:120536, ISSN 0957-4174, https://doi.org/10.1016/j.eswa.2023.120536
14. Da Silva Filho JI, Fernandes CLM, Silveira RS, Gomes PM, Matos SLC, Santo LE, et al. Process of Learning from Demonstration with Paraconsistent Artificial Neural Cells for Application in Linear Cartesian Robots. Robotics**.** 2023, 12,69. https://doi.org/10.3390/robotics12030069
15. De Carvalho A, Angelico BA, Justo JF, Oliveira AM, Da Silva Filho JI. Model reference control by recurrent neural network built with paraconsistent neurons for trajectory tracking of a rotary inverted pendulum, Appl. Soft Comput., 2023;133, 109927, ISSN 1568-4946, https://doi.org/10.1016/j.asoc.2022.109927
16. De Carvalho Jr A, Justo JF, Angélico BA, Oliveira AM, Da Silva Filho JI. Paraconsistent State Estimator for a Furuta Pendulum Control. SN Comput Sci. 2023. 4, 29. https://doi.org/10.1007/s42979-022-01427-z
17. De Carvalho Jr A, Justo JF, Angélico BA, de Oliveira AM, Da Silva Filho JI. Rotary Inverted Pendulum Identification for Control by Paraconsistent Neural Network, in IEEE Access. 2021;9:74155-67 doi: 10.1109/ACCESS.2021.3080176
18. Da Silva Filho JI, Cruz CM, Rocco A, Garcia DV, Ferrara LFP, Onuki AS, et al. Paraconsistent Artificial Neural Network for Structuring Statistical Process Control in Electrical Engineering. In: Akama, S. (eds) Towards Paraconsistent Engineering. Intell. Syst. Ref. Libr. 2016. vol 110. Springer, Cham. https://doi.org/10.1007/978-3-319-40418-9_6

19. Da Silva Filho JI, Caetano IS, Pontes FN, Mario MC, Abe JM, Giordano F. Paraconsistent Logic Algorithms Applied to Seasonal Comparative Analysis with Biomass Data Extracted by the Fouling Process. In: Abe, J. (eds) Paraconsistent Intelligent-Based Systems. Intell. Syst. Ref. Libr., vol 94. Springer, Cham. https://doi.org/10.1007/978-3-319-19722-7_6
20. Da Silva Filho JI. Treatment of Uncertainties with Algorithms of the Paraconsistent Annotated Logic. J Intell Learn Syst Appl, 2012;4(2):144-53. doi: 10.4236/jilsa.2012.42014
21. Toushmalani R. Comparison result of inversion of gravity data of a fault by particle swarm optimization and Levenberg-Marquardt methods. SpringerPlus 2. 2013;462. https://doi.org/10.1186/2193-1801-2-462